4-1-1996

Stability Analysis of a Model for the Defect Structure of YBa2Cu3Ox

Gregory Kozlowski
Wright State University - Main Campus, gregory.kozlowski@wright.edu

Tom Svobodny
Wright State University - Main Campus, thomas.svobodny@wright.edu

Stability analysis of a model for the defect structure of $YBa_2Cu_3O_x$

Gregory Kozlowski and Thomas Svobodny
Wright State University, Dayton, Ohio 45435
(Received 14 June 1995)

Unusual microstructures of $YBa_2Cu_3O_x$ (123) crystals have been observed. These structures have been shown to pass very high transport currents. A model of the solidification of 123 from a melt with Y_2BaCuO_5 (211) inclusions indicates that the stability of the 123 interface can depend on the sizes of the 211 inclusions. The observed formations are interpreted in the light of this instability.

I. INTRODUCTION

When $YBa_2Cu_3O_x$ (hereinafter, 123), is grown from the melt on a Y_2BaCuO_5 (211) substrate in the presence of Pt and CeO_2, unusual defects are observed that run parallel to the (100) and (010) planes. Experimental procedures and results pertaining to these defects were presented in Ref. 1 which also examined the evidence that an instability mechanism is responsible for the defect structure.

Figure 1 displays a sample sliced along a (001) plane. One sees clearly nonsolidified linear recesses of 10–20 μm in width and spaced about 100 μm apart. (We will refer to the part of the crystal between the recesses as an *arm*.) The arms extend in the [100] and [010] directions, that is, the ''*V*'' points in the [110] direction. In the arms can be seen the platelets parallel to (001) (Fig. 2). The recesses or gaps contain $BaCuO_2$ and CuO. Along the [110] diagonal are distributed 211 particles of size 1–5 μm. A pregrowth distribution of 211 particles can be seen on the back sides of the arms. The dominant size is about 2 μm. The distribution of 211, as one moves through the arm towards the front, shows a marked decrease in the size of the particles. As is seen in Fig. 2, the characteristic size of structures on the front is less than 1 μm, which is the characteristic platelet size. Figure 2 also shows how the observed platelet structure is, in this case, very fine.

This platelet structure is partially responsible for the anisotropy in critical current density. The nonsuperconducting phases that gather between platelets are one of the main factors in limiting transport currents in large specimens of 123. The periodic structures observed in Figs. 1 and 2 play the role of sink for unreacted liquid resulting in areas on one side of the arms with perfect monocrystalline structure. In this way, the current density is more isotropic and much larger transport currents can be achieved. For example, a 123 superconducting bar 12 cm in length was grown on a 211 substrate in the horizontal position, as described in Ref. 1. A current of 1500 A was passed the length of this bar, at the criterion of 1 μV/cm (Ref. 9). The longitudinal axis of the bar was (on the average) in the [001] direction, which supports the situation we have described.

It could be objected that crystals with this structure are mechanically weak, and liable to break down when carrying large currents. It has been found that nonreacting metals (such as Ag) can be added for strength. In that case the silver collects in the gaps between the arms and acts as structural reinforcement.

II. THE SOLIDIFICATION MODEL

An explanation for the size distribution can be arrived at by considering the mechanics of crystal growth. At first glance it would seem that Figs. 1 and 2 show a faceted dendritic growth. However, careful observation indicates that the true growth directions are not in accordance with that hypothesis. A (001) face grows via a spiral mechanism. The corners of the spiral correspond to the directions of fastest growth, in this case the [011]. Thus, in a local picture (a frame of reference moving with the front—which is, of course, not a material frame) the corner asserts itself like the prow of a ship. The smaller particles will be deflected by the boundary layer in the fluid, while the more massive particles will be less affected. According to the model of the solidification of 123 with peritectic reaction established by several groups,[2–4] the yttrium is supplied to the growing 123 (γ phase) front directly by 211 (α phase) inclusions via diffusion through the liquid, while diffusion of yttrium from solid inclusions of α phase in the γ phase is negligible. We can conclude then that the larger particles will be incorporated by the growing front and thereafter retain their size, while the fine particles that are pushed by the front will continue to supply the solute (yttrium). The observed spatial distribution of 211 particle size appears to hold the key. Larger particles are found along the joint of the arms and on the back side of the arms, smaller particles at the front of the arm. These

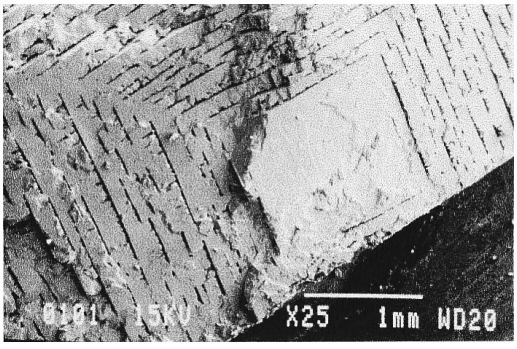

FIG. 1. Fracture surface micrograph of a melt process 123+Pt sample.

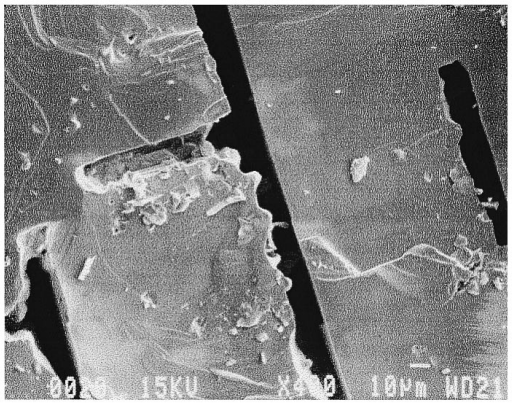

FIG. 2. Typical morphology of a 123+Pt single crystal grown by using a modified melt-textured technique or zone-melting method.

small particles, while being pushed by the growing front, continue to supply the solute. It does not seem reasonable to hold that the front stagnates due to an exhaustion of solute. This is confirmed by some results of Ref. 5 which found evidence of supersaturation at all times at the growing front.

The evidence[6–8,10] suggests that we look at the possibility that a morphological instability of the growing front plays an important role. In the present study, we show that the size distribution of inclusions does indeed effect the stability of the planar front. Our model addresses the response of the system to infinitesimal disturbances of an assumed steady growing planar front.

Although the solidification of 123 with peritectic reaction involves the three phases $\alpha(211)$, $\gamma(123)$, and liquid, mathematically we can treat it with a binary solidification model, since the process is limited by mass diffusion of the solute, yttrium, in the liquid, with the α particles acting as sources. The presence of these sources will give rise to boundary conditions in the mathematical model. Accordingly, we are interested in computing the growth rate of (small) perturbations to a steady planar growth of the γ phase where diffusion in the solid is absent.

The relevant parameters involved in the solidification are the diffusivity of yttrium in the liquid (D) (an important assumption of the model is that diffusivity in the solid is negligible), the steady growth rate of a planar front (V), the yttrium concentration in the liquid at the 123 interface (C_γ^L), the yttrium concentration in the 123 crystal at the interface (C_γ^S), the yttrium concentration in liquid at the 211 interface (C_α^L), the liquidus slope (m_γ, which is assumed constant), the melt temperature (T_m), and the capillary length (Γ). Table I displays the values that were used in the numerical calculations.

TABLE I. Values of parameters in the model.

D	10^{-6} cm^2/sec
V	3×10^{-5} cm/sec
C_γ^L	9.3×10^{-4} mol/cm^3
$k=C_\gamma^S/C_\gamma^L$	10
m	10^4 K cm^3/mol
$T_m\Gamma$	$(10^{-5},10^{-3})$ K cm

The main parameter of interest in the model is l, the 211 inclusion size. A major assumption in the analysis is that the particle size, l, is directly related to the inter-particle distance. Although a heterogeneous spatial distribution is apparent on the scale of the arms (1–100 μm), it can reasonably be supposed that, to first order, at the site of the planar front, the particles are uniformly distributed, so that the size parameter l is the characteristic separation distance. The uniform distribution of particles is brought about by mixing in the boundary layer. This is at scales larger than those relevant to the ensuing stability analysis.

III. STABILITY CALCULATION

In the mass diffusion limited situation above, we assume that as a planar front advances in a steady state, the temperature profile on either side of the front is linear, and that, in a moving frame, the concentration of yttrium, c, in the liquid satisfies

$$Dc_{zz}+Vc_z=0,$$

where the z direction is perpendicular to the moving front, which is found at $z=0$. The boundary conditions that apply in our model are

$$c|_{z=0}=C_\gamma^L, \quad c|_{z=l}=C_\alpha^L.$$

The resulting steady-state solution is

$$c(z)=C_\alpha^L\left(\frac{1-e^{-(V/D)z}}{1-e^{-(V/D)l}}\right)+C_\gamma^L\left(\frac{e^{-(V/D)z}-e^{-(V/D)l}}{1-e^{-(V/D)l}}\right). \quad (1)$$

If this solution is to be an equilibrium it should respect solute transport across the $z=0$ interface. This will lead to a relation between the parameters of the model, as discussed below. We suppose that the interface is perturbed sinusoidally in only one direction. The perturbation is given by $z=\phi(x)=\delta\sin\omega x$, where x is the coordinate along the front; ω and δ are the wave number and the (infinitesimal) amplitude of the disturbance. If we assume that the interface concentration in the liquid at the perturbed boundary is, to first order,

$$c_\phi^L=C_\gamma^L+\zeta\phi, \quad (2)$$

then the solution to the diffusion equation (in the liquid)

$$D(c_{xx}+c_{zz})+Vc_z=0 \quad (3)$$

that satisfies the appropriate boundary conditions is

$$c(x,z)=c(z)_v+\phi(x)(Ae^{-\omega_1 z}+Be^{-\omega_2 z}), \quad (4)$$

where

$$\omega_1=V/2D+\sqrt{(V/2D)^2+\omega^2}, \quad \omega_2=V/2D-\sqrt{(V/2D)^2+\omega^2} \quad (5)$$

and

$$A=\frac{(\zeta-G_c)e^{-\omega_2 l}}{e^{-\omega_2 l}-e^{-\omega_1 l}}, \quad B=-\frac{(\zeta-G_c)e^{-\omega_1 l}}{e^{-\omega_2 l}-e^{-\omega_1 l}}. \quad (6)$$

The term

$$G_c=\frac{V}{D}\frac{C_\alpha^L-C_\gamma^L}{1-e^{-(V/D)l}} \tag{7}$$

is a characteristic gradient of flux diffusion between the α and γ phases, adjusted for l. The effect of the perturbation on the temperature, T, is, to first order

$$T_\phi=T_m+C_\gamma^L m_\gamma+\theta\phi. \tag{8}$$

Three equations hold at the interface, the Gibbs-Thomson law, and two conservation laws; we will enforce these conditions to first order in δ; we will assume no solute diffusion in solid and ignore the variation of mass density. The Gibbs-Thomson law with constitutional supercooling is

$$T_\phi\simeq T_m+m_\gamma c_\phi^L-T_m\Gamma\kappa,$$

where κ is the curvature of the interface. The conservation of mass is

$$[c_\phi^L-c_\phi^S](V+\dot\phi)=-D\frac{\partial c}{\partial n}|_\phi, \tag{9}$$

where c_ϕ^S is the solute (yttrium) concentration in the solid (123) at the perturbed boundary. The conservation of energy is

$$L(V+\dot\phi)=-K_L\frac{\partial T}{\partial n}|_\phi+K_S\frac{\partial T}{\partial n}|_\phi,$$

where L is the latent heat of fusion of the 123 interface and K_L, K_S are thermal conductivities in liquid and solid phase, respectively. We have ignored the effect of undercooling on the latent heat, since this is not of first order in the shape of the front. We can use these relations to eliminate ζ, θ, and thereby obtain the disturbance growth rate, $\sigma=\dot\delta/\delta$. This growth rate for a disturbance of wave number ω has a dependence on l of the following form:

$$\sigma=2V\omega\left\{\frac{(-T_m\Gamma\omega^2-G_1)(\Omega+G_c/C_\gamma^L)+m(\Omega-V/D)}{2\omega m+G_2(\Omega+G_c/C_\gamma^L)}\right\}, \tag{10}$$

where

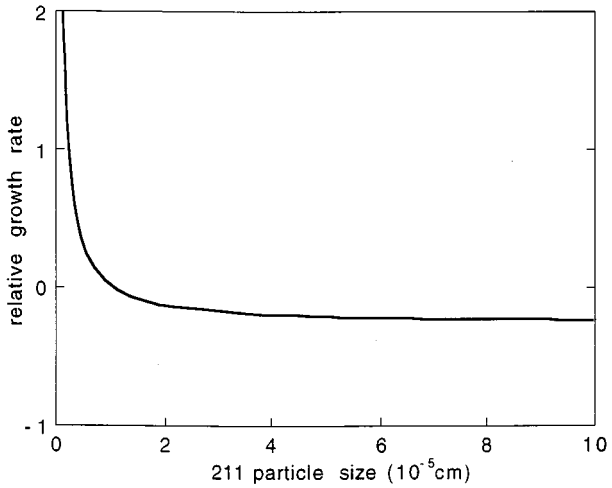

FIG. 3. Typical dependence of the growth rate of the planar front on sizes of 211 particle. Here the wave number is 10 000 cm^{-1}.

$$\Omega=V/2D+(\Delta\omega/2)\coth(l\Delta\omega/2), \tag{11}$$

and where $\Delta\omega=\omega_1-\omega_2$, $G_1+G_2=2K_Sg_S/(K_L+K_S)$, $G_1-G_2=2K_Lg_L/(K_L+K_S)$, and g_S, g_L are the thermal gradient on either side of the flat interface. Notice that (10) reduces to the usual Mullins-Sekerka formula in the limit of large l. For l on the order of the diffusion length, $l_d=D/V$, the range of unstable wave numbers decreases with decreasing l, and the growth rate σ does not change significantly. This has been alluded to in the literature. We will now proceed to demonstrate that the stability parameters change considerably for very small l (small compared to l_d).

When $l\omega\ll1$,

$$\Omega+G_c/C_\gamma^L\simeq V/2D+1/l+[d_0(1-e^{-(V/D)l})]^{-1},$$

where $d_0=D/(r-1)V$ is a reduced diffusion length and $r=C_\alpha^L/C_\gamma^L$. There are two characteristic length scales here. The diffusion scale $l_d=D/V$ has already been referred to. Now for $l\ll l_d$, using

$$[d_0(1-e^{-(V/D)l})]^{-1}\simeq(d_0lV/D)^{-1}=(r-1)/l,$$

the growth rate is

$$\sigma\simeq2V\omega\left\{\frac{-[r+(V/2D)l](T_m\Gamma\omega^2+G_1)+m[1-(V/2D)l]}{2\omega ml+G_2[r+(V/2D)l]}\right\}. \tag{12}$$

The solute-mass conservation (9) at zeroth order is

$$(k-1)(l/l_d)=(r-1), \tag{13}$$

and so, for small $l, r\approx1$. We define the marginally stable wave number ω_c by

$$\sigma(\omega_c,l)=0,\quad l\omega\ll1. \tag{14}$$

From (12), it can be seen that for reasonable choices of the parameters, ω_c can increase for decreasing l, and thus the range of unstable wave numbers can increase. In fact, since $G_1\ll m$, we have that, as $l\to0$,

$$\frac{d\omega_c}{dl}=-k(\omega_c^0/2l_d), \tag{15}$$

where ω_c^0 is the limiting critical wave number and is related to the parameters in the model as

$$\omega_c^0=\left(\frac{m}{T_m\Gamma}\right)^{1/2}.$$

Using the values in Table I, we have that the critical wavelength is between 10^{-4} and 10^{-5} cm. We can use this critical wave number to define the second important length scale, $l_p = G_2/2m\omega_c^0$. According to the values in Table I, this would be about 10^{-8} cm. As l approaches this length from above, the growth rate increases as $\sim 1/l$ (Fig. 3). Moreover, this growth rate is uniformly hyperbolic over the whole range of unstable wavelengths. To see this, note that in the range $l_p \ll l \ll I_d$, we have that the growth rate is

$$\sigma \simeq 2V\omega \left\{ \frac{-(T_m \Gamma \omega^2 + G_1) + m}{2\omega m l + G_2} \right\}. \tag{16}$$

It is important to notice that his range of l for which we have the hyperbolic disturbance growth rate is the range of sizes of 211 inclusions that is actually observed (Fig. 2).

We cannot make further predictions concerning eventual morphology, since the linear analysis does not pick out a distinguished wavelength. However, the range of unstable wavelengths is very large, which would seem to indicate a ''thickening'' of the surface area, leading to an energetic impediment to growth.

IV. CONCLUSION

A linear analysis of the response of disturbances to a growing planar front shows increased response as the parameter l is decreased, in both more wavelengths being affected as well as a greater disturbance growth rate; this supports the idea that an instability, in a yttrium-supersaturated growing front, in the presence of small size 211 particles, is the mechanism for the observed defect structures in textured 123. It may be expected that the equilibrium parameters, in particular V and D, may also be related to the parameter l. In an attempt to enforce this condition, we see from (9) that the term G_c/C_γ^L in (10) should incorporate some different l dependence; however, the term Ω will still be $1/l$, and the overall growth rate will still be $1/l$; we cannot expect this to change σ by more than an order of magnitude. The main conclusion is that growth rate of disturbances increases several orders of magnitude as l decreases over the relevant size range.

Further work on this problem will have to deal with both the 123 front and the kinetics of the included phase. This will necessarily involve a nonlinear stability analysis of a fully time-dependent model. Such a global model, which includes the convective mixing, is being developed. It should prove useful in the study of similar solidification reactions. In addition, further experimental work is needed to relate observable features of the interfacial structures to parameters in the model; this will allow a study of the control of structural features, such as the stem or arm area. Technology can benefit through larger superconductor transport currents.

[1] G. Kozlowski and T. Svobodny, Appl. Phys. Lett. **63**, 27 (1995).
[2] T. Izumi, Y. Nakamura, and Y. Shiohara, J. Mater. Res. **7**, 1621 (1992).
[3] M. J. Cima, M. C. Flemings, A. M. Figueredo, M. Nakade, H. Ishii, H. D. Brody, and J. S. Haggerty, J. Appl. Phys. **72**, 179 (1992).
[4] T. Izumi, Y. Nakamura, and Y. Shiohara, J. Cryst. Growth **128**, 1621 (1992).
[5] J. Ayache, P. Odier, and N. Pellerin, Supercond. Sci. Technol. **7**, 655 (1994).
[6] Y. Nakamura, K. Furuya, T. Izumi, and Y. Shiohara, J. Mater. Res. **9**, 1350 (1994).
[7] D. R. Uhlmann, B. Chalmers, and K. A. Jackson, J. Appl. Phys. **35**, 2986 (1964).
[8] C. Varanasi and P. J. McGinn, Physica C **207**, 79 (1993).
[9] G. Kozlowski (unpublished).
[10] B. N. Sun, P. Hartman, C. F. Woensdregt, and H. Schmid, J. Cryst. Growth **100**, 605 (1990).